ACS Chemical Neuroscience

Research Article

pubs.acs.org/chemneuro

Differential Effects of Structural Modifications on the Competition of Chalcones for the PIB Amyloid Imaging Ligand-Binding Site in Alzheimer's Disease Brain and Synthetic Aβ Fibrils

Marina Y. Fosso,[†] Katie McCarty,[‡] Elizabeth Head,[‡,§] Sylvie Garneau-Tsodikova,*[,†] and Harry LeVine, III*[,§,∥,⊥]

[†]Department of Pharmaceutical Sciences, College of Pharmacy, University of Kentucky, 789 South Limestone Street, Lexington, Kentucky 40536-0596, United States

[‡]Department of Pharmacology and Nutritional Sciences, [§]Center on Aging, [∥]Molecular and Cellular Biochemistry, and [⊥]Center for Structural Biology, School of Medicine, University of Kentucky, Lexington, Kentucky 40536-0230, United States

Supporting Information

ABSTRACT: Alzheimer's disease (AD) is a complex brain disorder that still remains ill defined. In order to understand the significance of binding of different clinical in vivo imaging ligands to the polymorphic pathological features of AD brain, the molecular characteristics of the ligand interacting with its specific binding site need to be defined. Herein, we observed that tritiated Pittsburgh Compound B (^{3}H-PIB) can be displaced from synthetic Aβ(1−40) and Aβ(1−42) fibrils and from the PIB binding complex purified from human AD brain (ADPBC) by molecules containing a chalcone structural scaffold. We evaluated how substitution on the chalcone scaffold alters its ability to displace ^{3}H-PIB from the synthetic fibrils and ADPBC. By comparing unsubstituted core chalcone scaffolds along with the effects of bromine and methyl substitution at various positions, we found that attaching a hydroxyl group on the ring adjacent to the carbonyl group (ring I) of the parent member of the chalcone family generally improved the binding affinity of chalcones toward ADPBC and synthetic fibrils F_{40} and F_{42}. Furthermore, any substitution on ring I at the *ortho*-position of the carbonyl group greatly decreases the binding affinity of the chalcones, potentially as a result of steric hindrance. Together with the finding that neither our chalcones nor PIB interact with the Congo Red/X-34 binding site, these molecules provide new tools to selectively probe the PIB binding site that is found in human AD brain, but not in brains of AD pathology animal models. Our chalcone derivatives also provide important information on the effects of fibril polymorphism on ligand binding.

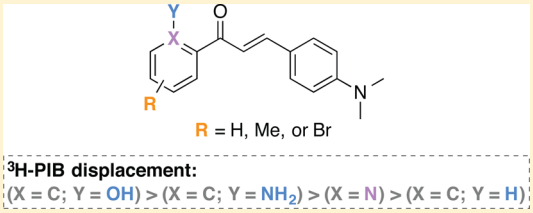

KEYWORDS: *Displacement assay, neurodegenerative disorder, Pittsburgh compound B, radioactive assay, structure−activity relationships*

In 2004 the benzothiazole aniline Aβ amyloid fibril ligand Pittsburgh Compound B (PIB) labeled with ^{11}C for positron emission tomography (PET) imaging was shown in a small study of living patients to be retained in brain areas known to accumulate Aβ pathology in Alzheimer's disease (AD) brains, but not in normal brains.[1] Subsequent studies showed that PIB uptake tracked with disease progression starting decades before cognitive symptoms were evident.[2,3] As the most widely clinically used Aβ deposition tracer, PIB is generally considered a benchmark for amyloid PET imaging agents.

The effort to find agents for early diagnosis of AD by imaging Aβ pathology in living patients has produced a variety of small molecule and peptide ligands (reviewed in ref 4). While many such molecules have been identified, little is known about which features of Aβ pathology are being reported and which ligands are recognizing the same feature or binding to the same site. Lockhart and colleagues defined distinct sites for ligands on synthetic Aβ fibrils based on their ability to compete for binding.[5,6] Other studies elaborated and confirmed the concept of multiple distinct sites on Aβ fibrils for ligands to bind.[7,8]

The significance of this multiplicity of ligand-binding sites was brought into sharp focus by the initial observation by Klunk and co-workers that the benzothiazole aniline ligand PIB bound with high affinity in large amounts to AD brain, but only very little bound to similar amounts of Aβ pathology in a transgenic mouse model of AD.[9] High affinity ^{3}H-PIB binding was also negligible in other genetic and natural nonhuman primate and canine animal models of AD Aβ pathology.[10] By contrast, ligands such as Congo Red and X-34 (Scheme 1D), which do not compete for PIB binding and, therefore, bind to a site distinct from where PIB binds to Aβ pathology, bound normally in these animal models. Since humans are the only animal that suffers the full progression of AD, these findings suggested that the site to which PIB binds was unique and that elucidation of how it was formed and its structure might provide insight into the disease process and potential therapeutic avenues. Our determination that PIB

Received: October 7, 2015
Accepted: December 18, 2015
Published: December 18, 2015

DOI: 10.1021/acschemneuro.5b00266
ACS Chem. Neurosci. 2016, 7, 171−176

Scheme 1[a]

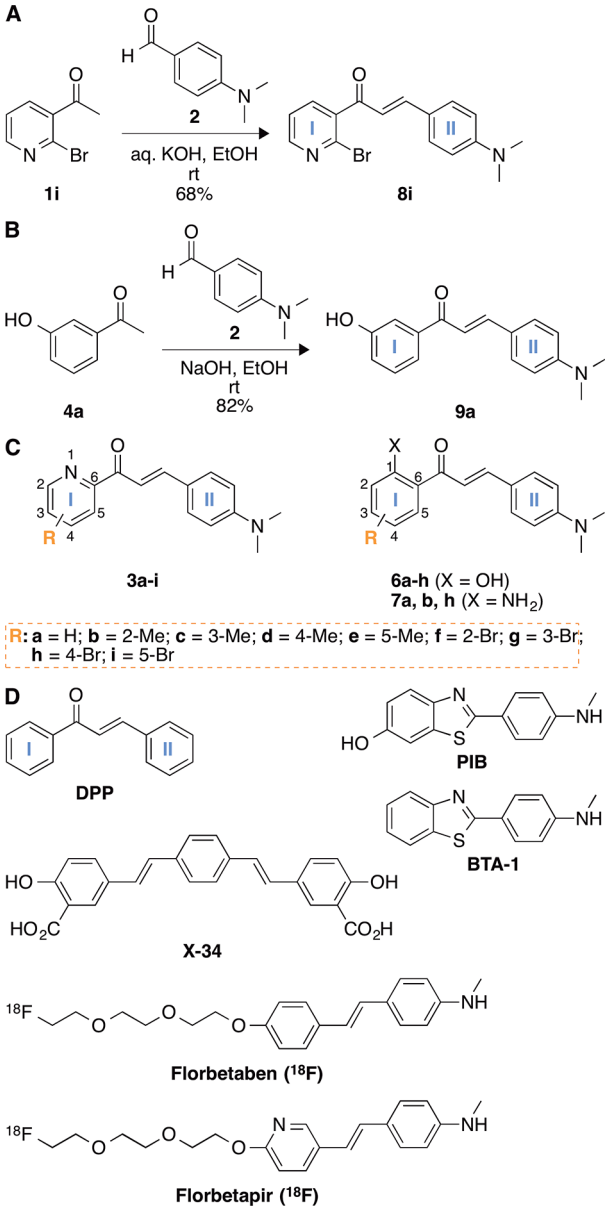

[a]Synthetic scheme for the preparation of (A) chalcone **8i** and (B) chalcone **9a**. (C) Structures of chalcones **3a**−**i**, **6a**−**h**, and **7a**, **b**, **h**. (D) Structures of DPP, PIB, BTA-1, X-34, florbetaben (^{18}F), and florbetabir (^{18}F).

binding Aβ pathology was an isolatable fraction of the total AD brain Aβ pathology with different physical properties and protein composition[11] indicated that high affinity PIB binding addressed a reasonably discrete population of peptide conformers present at high levels in human AD brain and only low levels in animal models.

These observations suggest that imaging ligands that bind to Aβ pathology at sites distinct from the PIB binding site have the potential to be reporting different processes or to miss events, both of which would foster confusion potentially leading to misinterpretation in diagnosis and in defining progression mechanisms. Ni and colleagues showed in AD tissue homogenates that the two ^{18}F-labeled stilbene derivatives florbetapir (Amyvid) and florbetaben (Neuraceq) (Scheme 1D) now used in the clinic, compete for PIB binding to AD brain tissue, as does Vizamyl (flutemetamol; 2-[3-[^{18}F]fluoro-4-(methylamino) phenyl]-6-benzothiazolol), a PIB derivative.[12] Thus, imaging in AD brain with these ligands should give similar results to those with ^{11}C-PIB.

PIB competition results have not been reported for the majority of ligands shown in preclinical studies to bind Aβ pathology. Based on the fact that the chalcone scaffold (1,3-diphenyl-2-propen-1-one, DPP, Scheme 1D) highly resembles the florbetaben and florbetapir core, with the exception of the additional carbonyl group in DPP, and also based on the fact that the *N*,*N*-dimethylamino/*N*-monomethylamino moieties of various molecules have been demonstrated to be critical to Aβ binding, we hypothesized that chalcone dertivatives containing an *N*,*N*-dimethylamino group could potentially compete for the PIB binding site in Aβ. Here, we demonstrate that molecules based on the chalcone scaffold displace ^{3}H-PIB from the Alzheimer's disease PIB binding complex (ADPBC) purified from AD brain, as well as from more widely available model fibrils assembled from synthetic Aβ(1−40) and Aβ(1−42) peptides. We also show that a prototypical chalcone of our series, **9a**, stains Aβ plaque pathology selectively, and like PIB, does not stain tau pathology in tissue sections from hippocampus of AD brain. Several series of electron-withdrawing, electron-donating, and bulky substituents on ring I produced molecules with EC_{50} values displaying consistent structure−activity relationships (SAR). ^{3}H-X-34 binding was unaffected by these chalcones (EC_{50} values > 10 μM). Quantification of ^{3}H-PIB binding to synthetic peptide Aβ(1−40) and Aβ(1−42) fibrils (indicated from here on as F_{40} and F_{42}, respectively) indicated a high Aβ:PIB stoichiometry, many Aβs per high affinity PIB binding site, while the purified ADPBC from AD brain showed nearly a 1:1 stoichiometry.[10]

We report that the SAR of chalcones for synthetic F_{40} and F_{42} fibrils differs from that of the AD brain site, and that the F_{40} and F_{42} fibrils have SARs distinct from one another. This suggests that the details of the binding site for chalcones that compete for PIB binding differ among the different fibril populations.

RESULTS AND DISCUSSION

Chemistry. Chalcones have long been known as a prolific class of compounds, displaying a vast array of biological activities.[14] With the aim of investigating their effects on the formation and dissociation of Aβ oligomers, we recently reported on the synthesis of three series of chalcones,[15] differing from each other by the nature of ring I (Scheme 1C). They bear either a pyridine (compounds **3a**−**i**), a phenol (compounds **6a**−**h**), or an aniline (compounds **7a**, **b**, **h**) moiety as ring I. Electron-withdrawing, electron-donating, and bulky substituents, such as a methyl or a bromo group, were also introduced at various positions on ring I. We further expanded this series of chalcones by including compounds **8i** (Scheme 1A) and **9a** (Scheme 1B), which were obtained in 62 and 86% yields, respectively, by reacting 4-(dimethylamino)benzaldehyde, **2**, with the corresponding ketone (**1i** and **4a**, respectively) in the presence of a base (KOH or NaOH). Overall, the modifications on ring I were selected with the goals of (i) mimicking the pyridine ring of florbetapir and (ii) attaching handles that we could later potentially use to further derivatize our molecules and generate radiolabeled or fluorescently labeled compounds as imaging agents.

Investigation of Unsubstituted Core Scaffolds. After establishing that our chalcones did not compete for binding with ^{3}H-X-34 (all EC_{50} values against ^{3}H-X-34 > 10 μM), we investigated the binding of the unsubstituted core scaffolds

DOI: 10.1021/acschemneuro.5b00266
ACS Chem. Neurosci. 2016, 7, 171−176

Table 1. EC_{50} Values (μM) of Chalcone Competition for ^{3}H-PIB Binding to Aβ Preparations[a]

					ratio of EC_{50} values[b]		
entry	compd	F_{40}	F_{42}	ADPBC	F_{40}/F_{42}	F_{40}/ADPBC	F_{42}/ADPBC
1	**3a**	1.150 ± 0.071	0.350 ± 0.057	0.037 ± 0.005	3.3	31	9.5
2	**3b**	4.200 ± 0.283	1.850 ± 0.636	>10	2.3	[c]	[c]
3	**3c**	2.100 ± 0.707	0.097 ± 0.005	0.465 ± 0.078	22	4.5	0.2
4	**3d**	>10	0.125 ± 0.007	0.013 ± 0.001	[c]	[c]	10
5	**3e**	5.100 ± 1.556	3.700 ± 0.707	6.050 ± 1.344	1.4	0.8	0.6
6	**3f**	1.150 ± 0.071	0.555 ± 0.021	0.795 ± 0.035	2.1	1.4	0.7
7	**3g**	0.765 ± 0.049	0.105 ± 0.007	0.142 ± 0.069	7.3	5.4	0.7
8	**3h**	0.515 ± 0.120	0.026 ± 0.006	0.008 ± 0.001	20	64	3.3
9	**3i**	9.000 ± 1.414	4.300 ± 1.414	8.000 ± 1.414	2.1	1.1	0.5
10	**6a**	0.030 ± 0.004	0.120 ± 0.028	0.010 ± 0.003	0.3	3	12
11	**6b**	0.083 ± 0.014	0.063 ± 0.010	0.009 ± 0.003	1.3	9.2	7.0
12	**6c**	0.058 ± 0.001	0.110 ± 0.014	0.056 ± 0.021	0.5	1.0	2.0
13	**6d**	0.570 ± 0.339	0.170 ± 0.042	0.185 ± 0.035	3.4	3.1	0.9
14	**6e**	2.250 ± 0.212	1.800 ± 0.849	1.650 ± 0.071	1.3	1.4	1.1
15	**6f**	0.150 ± 0.014	0.125 ± 0.007	0.014 ± 0.004	1.2	11	8.9
16	**6g**	0.050 ± 0.000	0.410 ± 0.014	0.032 ± 0.001	0.1	1.6	13
17	**6h**	0.220 ± 0.014	0.520 ± 0.028	0.150 ± 0.042	0.4	1.5	3.5
18	**7a**	0.035 ± 0.006	0.110 ± 0.014	0.059 ± 0.002	0.3	0.6	1.9
19	**7b**	0.270 ± 0.085	0.082 ± 0.040	0.010 ± 0.002	3.3	27	8.2
20	**7h**	1.050 ± 0.071	0.675 ± 0.078	>10	1.6	[c]	[c]
21	**8i**	>10	9.000 ± 1.414	>10	[c]	[c]	[c]
22	**9a**	0.165 ± 0.064	0.036 ± 0.008	0.013 ± 0.001	4.6	13	2.8
23	DPP	9.500 ± 0.707	1.750 ± 0.495	0.650 ± 0.071	5.4	15	2.7
24	PIB	0.015 ± 0.007	0.040 ± 0.005	0.003 ± 0.001	0.4	4.3	11.6
25	BTA-1	0.026 ± 0.007	0.031 ± 0.002	0.003 ± 0.001	0.8	8.8	10.5

[a] F_{40} = Aβ(1−40) fibrils; F_{42} = Aβ(1−42) fibrils; ADPBC = PIB binding site isolated from AD brain (see Methods). [b] Large or small ratios indicate that the compound binds differently to each fibril type, whereas ratios close to 1 indicate compounds with comparable affinity to the fibril types compared. [c] Due to solubility-micellarization concerns which interfere with ^{3}H-PIB binding measurements, compounds were not tested at concentrations greater than 10 μM and no ratio can be calculated in this case.

(DPP, **3a**, **6a**, **7a**, and **9a**) to ADPBC. The parent member of the chalcone family, DPP (Scheme 1D), was first evaluated, and it was found to have better affinity for displacing ^{3}H-PIB from ADPBC than synthetic F_{40} and F_{42} fibrils (Table 1, entry 23). While not as potent as the best benzothiazole aniline ligands (PIB, EC_{50} = 2.6 nM; BTA-1, EC_{50} = 3 nM),[11] it was submicromolar despite missing the *N*,*N*-dimethylamino/*N*-monomethylamino moiety on the aromatic ring critical for the benzothiazole aniline ligands.[16]

Selectivity of Chalcone Scaffold for AD Brain Aβ Plaque Pathology. Sections of hippocampal tissue from AD brain containing both Aβ plaque pathology and tau neurofibrillary tangle pathology were stained with chalcone **9a** to verify its selectivity for the Aβ pathology (Figure 1). Thioflavin S stains both Aβ plaques (white triangles) and tau pathology (white arrows) in panel **A**. By contrast, like PIB and its analogue 6-CN-PIB, the chalcone stains only the Aβ plaque pathology (white triangles) in an adjacent tissue section shown in panel **B**. This selectivity convinced us of the potential ability of chalcones to effectively displace PIB from its binding site in AD brain and in synthetic peptide model systems, and led us to investigate the effects of substitution on the structural scaffold of DPP. The ratios of EC_{50} values shown in Table 1 for displacement of ^{3}H-PIB from the different Aβ fibril sources also provide insight into the relative similarity of the ligand-binding site on those fibrils. Large or small ratios indicate that the compound binds differently to each type of fibrils, whereas ratios close to 1 indicate compounds with comparable affinity to the types of fibrils compared.

Upon attachment of a *N*,*N*-dimethylamino moiety on ring II and replacement of the benzene ring I in DPP by a pyridine (**3a**, entry 1), phenol (**6a**, entry 10), or aniline (**7a**, entry 18) moiety, we observed that the core scaffold **6a** binds better than the core scaffold **3a**, which in turn binds better than DPP to ADPBC, F_{40}, and F_{42} fibrils. Furthermore, **6a** and **7a** have comparable binding affinity toward F_{40} and F_{42} fibrils, but the core scaffold **7a** does not bind as well as **6a** and **3a** to ADPBC. It thus appears that having a phenol as ring I provides the strongest competitor to ^{3}H-PIB in ADPBC, F_{40}, and F_{42} fibrils, while the presence of the benzene ring alone imparted the weakest displacement of ^{3}H-PIB in all cases. Furthermore, when the hydroxyl group on **6a** was moved away from position 1 to 2, as in **9a** (Table 1, entry 22), the binding affinity and fibril selectivity were altered. Compound **6a** was better than **9a** at binding synthetic F_{40} fibrils, while the opposite was observed for synthetic F_{42} fibrils. Not surprisingly though, the EC_{50} values for the two compounds were similar in ADPBC, which may reflect the additional components (lipids, other proteins) in the ADPBC. As a result, we decided to pursue our structural modifications on ring I of core scaffolds **3a**, **6a**, and **7a**.

Direct Comparison of Methylated and Brominated Core Scaffolds. By adding a methyl or bromo group at positions 2−5 of ring I, we were able to compare chalcone derivatives with the same substituent at the same position in that ring. In the presence of F_{40} fibrils, the EC_{50} values of chalcone derivatives **6a**−**h** (Figure 2B) with the phenol ring (entries 10−17) were the smallest (highest affinity), in comparison to **3a**−**h** (Figure 2A) with a pyridine moiety (entries 1−8) and **7a**, **b**, and **h** with an

DOI: 10.1021/acschemneuro.5b00266
ACS Chem. Neurosci. 2016, 7, 171−176

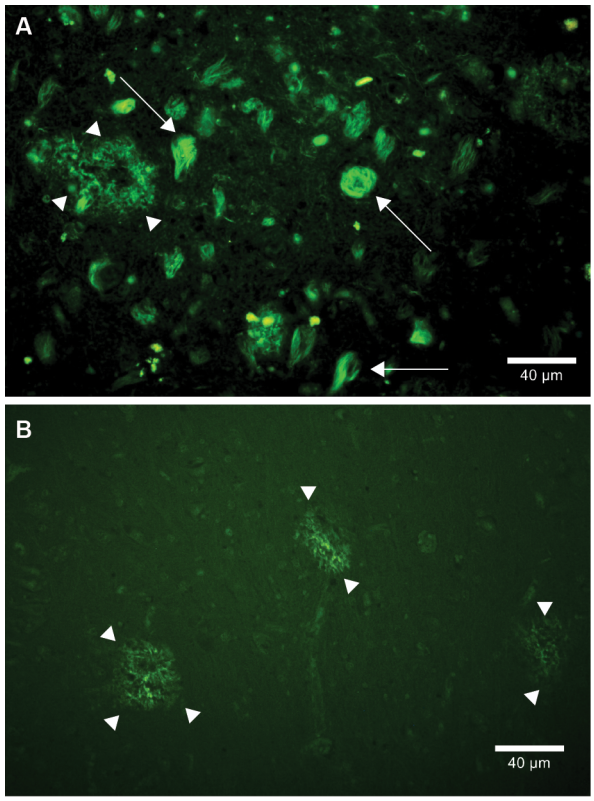

Figure 1. Thioflavin S and chalcone **9a** labeling in the hippocampus of an AD case. (A) Thioflavin S binds to plaques (white triangles) and neurofibrillary tangles (white arrows) in area CA1 of the hippocampus. (B) In contrast, chalcone **9a** binds to plaques (white triangles), but not neurofibrillary tangles in an adjacent section from the same case. Scale bar = 40 μm.

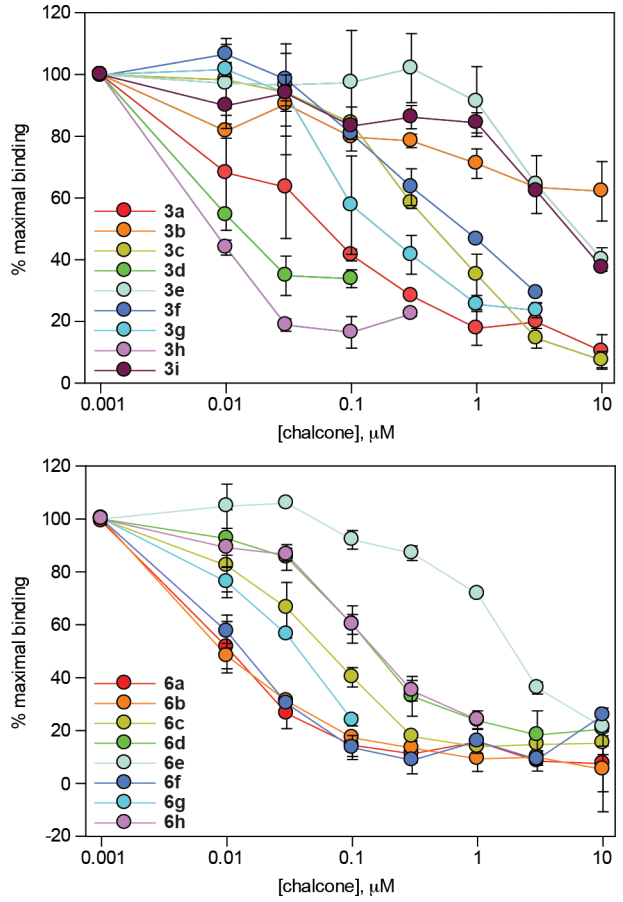

Figure 2. Displacement of ^{3}H-PIB from ADPBC by (A) chalcones **3a**–**i** and (B) chalcones **6a**–**h**. Percent maximal ^{3}H-PIB binding = (binding in absence of competitor − binding in the presence of 1 μM BTA-1). Mean of two assays on separate days ± SD.

aniline (entries 18–20). In the case of F_{42} fibrils, any substitution at position 2 or 5 will still make the chalcone derivatives with the phenolic ring (entries 11, 14, and 15) better (lower EC_{50}, higher affinity) than their corresponding analogues with the pyridine (entries 2, 5, and 6). On the other hand, if a methyl group is at position 3 or 4, the chalcone derivatives from the pyridine (scaffold **3**; entries 3–4) and phenol (scaffold **6**; entries 12–13) series have comparable affinities; meanwhile, a bromo group at position 3 or 4 will make the chalcone derivatives with a pyridine moiety (entries 7–8) better competitor than the ones with the phenol (entries 16–17). It thus appears that the presence of a weak electron-withdrawing group (EWG) at position 3 or 4 will switch which one is better in F_{42} fibrils. In the case of ADPBC, substitution did not seem to have a large effect, since the chalcone derivatives with the phenol moiety had higher affinity than their counterparts with a pyridine or an aniline moiety, with the exception of **6d** (entry 13) and **6h** (entry 17), which had higher EC_{50} values (lower affinity) than their respective pyridine analogues **3d** (entry 4) and **3h** (entry 8). Overall, **6a**–**h** with the phenol moiety had higher affinity for ADPBC, F_{40}, and F_{42} fibrils (Table 1, entries 10–17) than their counterparts with a pyridine (**3a**–**h**, entries 1–8) or an aniline moiety (**7a**, **b**, and **h**, entries 18–20), which confirms our initial findings that having a phenol moiety as ring I conferred higher affinity binding to ADPBC, F_{40}, and F_{42} fibrils. It is important to note that, although not in all cases, overall, the more lipophilic compounds (higher log *P* values in Table S1) displayed higher binding affinity to Aβ.

Comparison of the Effect of Bromine versus Methyl Substitution. When comparing the methyl group versus the bromo group as substituents on ring I, it appears that the chalcone derivatives with the bromo group display comparable or higher affinity than their methyl counterparts toward ADPBC, F_{40}, and F_{42} fibrils, with the exception of **6f** (entry 15), **6g** (entry 16), and **6h** (entry 17), which did not bind synthetic F_{42} fibrils as well as their methyl counterparts **6b** (entry 11), **6c** (entry 12), and **6d** (entry 13), respectively. This suggests that a weak EWG such as a bromo group might enhance the binding affinity of the chalcones.

Comparison of the Effect of Substitution Pattern on Core Scaffolds. Regarding the effect on binding affinity of various positions for substitution on ring I of all three core scaffolds (**3**, **6**, and **7**), we noticed that, for synthetic F_{40} fibrils, position 3 was generally preferred over position 2, which in turn was preferred to position 4. In the case of ADPBC and F_{42} fibrils, position 2 was generally preferred over position 3, which in turn was preferred to position 4 for the chalcone derivatives with the phenol moiety. Overall, position 5 appears to be the least favored in most cases, probably due to the steric hindrance that might be created. We also observed that moving the nitrogen of the pyridine ring away from the carbonyl moiety of the chalcone, as in compound **8i** (entry 21), is disfavored and series **8** was therefore not further investigated.

Previous SAR with the benzothiazole aniline series[11,16] suggests a relatively sterically restricted binding pocket with a

DOI: 10.1021/acschemneuro.5b00266
ACS Chem. Neurosci. 2016, 7, 171–176

parallel SAR for ADPBC, F_{40}, and F_{42} fibrils. The more flexible chalcone scaffold is relatively tolerant of substituents. Interestingly, the chalcone derivatives investigated here markedly distinguish among the ADPBC, F_{40}, and F_{42} fibrils. This behavior could reflect a different binding mode for chalcones, which probes the structural organization of the fibrils around while occluding a subsite that binds the benzothiazole aniline moiety. Chalcones could be especially sensitive to Aβ fibril polymorphism around the PIB binding site, which is distinct from the pan-amyloid fibril-binding site for Congo Red and X-34.

CONCLUSIONS

In summary, we found that the chalcone scaffold widely reported as Aβ imaging tracers[4] competes for ^{3}H-PIB binding, but not for ^{3}H-X-34 binding to synthetic Aβ(1−40) and Aβ(1−42) fibrils and to the PIB-binding fraction of Aβ isolated from AD brain. As hypothesized, exploration of a series of ring I substitutions revealed a consistent pattern of differential effects on competition for ^{3}H-PIB binding that differentiated the two synthetic peptide fibrils from each other as well as from the AD brain material. Overall, the pattern of the EC_{50} values of chalcone displacement of ^{3}H-PIB from PIB binding fraction from AD brain most closely resembled that of the synthetic Aβ(1−42) fibrils (Table 1). Since the chalcones studied did not interact with the Congo Red/X-34 binding site, they provide tools to explore details of Aβ fibril structure around the PIB binding pocket and effects of fibril polymorphism on ligand binding, which may explain the low binding of PIB to the Aβ pathology of animal models.

METHODS

Materials and Instrumentation. Human autopsy tissue for preparation of the ADPBC was obtained from the University of Kentucky Center on Aging Brain Bank of the Alzheimer's Disease Center in accordance with federal and institutional IRB guidelines with informed consent, and samples were deidentified to ensure the anonymity of subjects. The study conforms to The Code of Ethics of the World Medical Association. All chemicals were purchased from Sigma-Aldrich (St. Louis, MO) and used without further purification. Chemical reactions were monitored by thin layer chromatography (TLC) using Merck silica gel 60 F_{254} plates. Visualization was achieved using UV light and $KMnO_4$ stain (1.5 g $KMnO_4$, 10 g K_2CO_3, 1.25 mL 10% NaOH, 200 mL H_2O). ^{1}H and ^{13}C NMR spectra were recorded at 400 and 100 MHz, respectively, on a Varian 400 MHz spectrometer, using the indicated solvents. Chemical shift (δ) is given in parts per million (ppm). Coupling constants (J) are given in hertz (Hz), and conventional abbreviations used for signal shape are as follows: s = singlet; d = doublet; t = triplet; m = multiplet; dd = doublet of doublets; dt = doublet of triplets. Liquid chromatography−mass spectrometry (LCMS) was carried out using an Agilent 1200 series Quaternary LC system equipped with a diode array detector, and Eclipse XDB-C_{18} column (250 mm × 4.6 mm, 5 μm), and an Agilent 6120 Quadrupole MSD mass spectrometer (Agilent Technologies, Santa Clara, CA). LCMS M + H signals were consistent with the expected molecular weights for all of the reported compounds.

Synthesis of Chalcone Ligands. The synthesis and structural characterization of chalcones **3a**−**i**, **6a**−**h**, and **7a**, **b**, **h** were performed as previously described.[15]

*Synthesis of Chalcone **8i**.* A solution of 3-acetyl-2-bromopyridine (**1i**) (201 mg, 1.0 mmol) and 4-(dimethylamino)benzaldehyde (**2**) (150 mg, 1.0 mmol) in EtOH (5 mL) was treated with 3 mL of a 20% aqueous KOH solution and allowed to stir at rt for 3 h. Upon completion of the reaction, H_2O (5 mL) was added and the solid residues that formed were filtered out, rinsed with H_2O and ice-cold EtOH, and recrystallized from CH_2Cl_2/hexanes to give compound **8i** (R_f 0.17 in hexanes/EtOAc 3:1) as dark yellow needles (226 mg, 68% yield): ^{1}H NMR (400 MHz, $CDCl_3$) δ 8.46 (dd, J_1 = 4.8 Hz, J_2 = 2.0 Hz, 1H, aromatic), 7.70 (dd, J_1 = 7.2 Hz, J_2 = 2.0 Hz, 1H, aromatic), 7.46 (dt, J_1 = 9.2 Hz, J_2 = 2.0 Hz, 2H, aromatic), 7.36 (d, J = 15.6 Hz, 1H, HC = C<u>H</u>-Ph), 7.37 (dd, J_1 = 7.2 Hz, J_2 = 4.8 Hz, 1H, aromatic), 6.89 (d, J = 15.6 Hz, 1H, <u>H</u>C = CH-Ph), 6.69 (dt, J_1 = 9.2 Hz, J_2 = 2.0 Hz, 2H, aromatic), 3.05 (s, 6H, N(C<u>H</u>$_3$)$_2$). ^{13}C NMR (100 MHz, $CDCl_3$) δ 192.7, 152.5, 150.6, 148.8, 138.9, 138.7, 137.4, 130.9 (2 carbons), 122.5, 121.6, 120.4, 111.8 (2 carbons), 40.1 (2 carbons). m/z calcd for $C_{16}H_{15}BrN_2O$, 330.0; found, 331.0 $[M + H]^+$.

*Synthesis of Chalcone **9a**.* The known compound **9a** was prepared as previously described.[19] A solution of 3′-hydroxy acetophenone (**4a**) (68 mg, 0.5 mmol) and 4-(dimethylamino)benzaldehyde (**2**) (75 mg, 0.5 mmol) in EtOH (1.5 mL) was treated with NaOH pellets (400 mg, 10.0 mmol). The reaction was stirred at rt overnight until completion. Most of the solvent was then removed, and 1 N aqueous HCl was added. The precipitate was filtered to give the known compound **MFY-4−8** (R_f 0.26 in hexanes/EtOAc 3:1) as an orange solid (110 mg, 82% yield): ^{1}H NMR (400 MHz, $CDCl_3$, which matches the lit.[19]) δ 7.78 (d, J = 15.6 Hz, 1H, HC = C<u>H</u>-Ph), 7.56−7.50 (m, 4H, aromatic), 7.35 (t, J = 8.0 Hz, 1H, aromatic), 7.29 (d, J = 15.6 Hz, 1H, <u>H</u>C = CH-Ph), 7.03 (dd, J_1 = 8.0 Hz, J_2 = 2.0 Hz, 1H, aromatic), 6.69 (d, J = 9.2 Hz, 2H, aromatic), 5.30 (s, 1H, O<u>H</u>), 3.04 (s, 6H, N(C<u>H</u>$_3$)$_2$).

Preparation of Aβ Fibrils. AD brain ADPBC was purified from autopsy human AD frontal cortex as previously described[11] and was stored in aliquots at −75 °C. For the recombinant Aβ (rPeptide, Bogart, GA) 1 mg each of Aβ(1−40) (cat. A-1153−2, lot #6050840H) and Aβ(1−42) (cat. A-1163−2, lot #4230842H) obtained as films dried from HFIP were dissolved in 900 μL of ice-cold distilled H_2O and kept on ice for 30 min with intermittent vortexing. A volume of 100 μL of 10× PBS (final concentration 20 mM sodium phosphate, 145 mM NaCl, pH 7.4) was added with vortexing followed by 20 μL of 2% w/v NaN_3. The solutions were transferred to separate screw cap polypropylene tubes, sealed, and incubated at 37 °C for 1 week, vortexing briefly once each day. Fibril formation was assessed by sedimentable Thioflavin T fluorescence.[13,17] Aliquots of fibrils (1 mg/mL) were frozen at −20 °C and thawed immediately before use.

Radioligand Binding Assays. *^{3}H-PIB Binding.* ^{3}H-PIB binding was assessed in Aβ preparations from AD brain and in fibrils prepared from Aβ(1−40) and Aβ(1−42) recombinant peptides (F_{40} and F_{42}, respectively).[11] For binding studies, 20 μL of PBS containing purified ADPBC equivalent to 133.3 μg wet weight of original tissue, 100 ng of F_{40}, or 50 ng of F_{42} was added to each of duplicate wells of a 96-well polypropylene plate (Costar 3365). Under the conditions of the assay, these quantities of Aβ gave similar total amounts of ^{3}H-PIB binding, 10−15% of the input radioactivity. A volume of 200 μL of 1.2 nM ^{3}H-PIB (cat. VT 278 specific radioactivity = 70.2 Ci/mmol, Vitrax (Placentia, CA)) containing a dose response of nonradioactive competitor at a final concentration of DMSO of 1% v/v in PBS + 5% v/v EtOH was added to each well. Samples were incubated for 3 h at room temperature without shaking, transferred to a 96-well Millipore Multiscreen HTS Hi Flow FB (GF/B) filter plate, and filtered on a multiwell plate vacuum manifold (Millipore Corporation, Bedford, MA). The filters were rapidly washed three times with 200 μL of PBS + 5% v/v EtOH, dried, removed from the plate, and placed in scintillation vials. A volume of 2 mL of BudgetSolve scintillation fluid was added, and the vials capped and shaken before counting for ^{3}H in a Packard TriCarb 2500 TR scintillation counter. Specific binding was calculated as (mean CPM of the two filters from wells containing radioactive PIB + competitors) minus (CPM value from wells containing radioactive PIB + 1 μM nonradioactive BTA-1 competitor). EC_{50} values were determined by titrating increasing concentrations of unlabeled test compound against constant (1.3 nM) ^{3}H-PIB. The EC_{50} is the concentration at which 50% of the specifically bound ^{3}H-PIB is displaced. Although the EC_{50} values are slightly greater than the IC_{50} values because more than 10% of the total radioligand is bound, the EC_{50} values can be compared with each other since they were determined under the same conditions.

^{3}H-X-34 Binding. ^{3}H-X-34 binding[18] was performed similarly to PIB binding with 5 nM ^{3}H-X-34, 23 Ci/mmol, custom tritiated by Vitrax (Placentia, CA)) with 10 μM X-34 or Congo Red as nonradioactive X-34 competitor.

DOI: 10.1021/acschemneuro.5b00266
ACS Chem. Neurosci. 2016, 7, 171−176

Chalcone and Thioflavin S Histochemistry. Formalin-fixed hippocampal sections from an AD case (77 year old female, Braak VI, postmortem interval 4.15 h, ApoE 4/4), 8 μm thick were deparaffinized and rehydrated through decreasing concentrations of alcohol until washing in PBS. Sections were incubated in a room temperature humidifier with 2 mM chalcone **9a** in 20% v/v DMSO in PBS for 1 h in the dark. After 3 × 1 min PBS washes, sections were treated with TrueBlack Lipofuscin Autofluorescence Quencher (30s-Biotium, Hayward, CA) and then coverslipped using Everbrite Hardset Mounting Medium (Biotium, Haywad, CA). An adjacent section was stained with thioflavin S (0.5% w/v in 50% v/v EtOH) for 5 min, then washed in 50% EtOH, followed by ddH_2O, and then coverslipped using Vectashield with DAPI (Vector Laboratories, Burlingame, CA). Images were captured using an Olympus BX51 fluorescence microscope with a wide band-pass filter.

■ ASSOCIATED CONTENT

Supporting Information

The Supporting Information is available free of charge on the ACS Publications website at DOI: 10.1021/acschemneuro.5b00266.

^{1}H and ^{13}C NMR spectra for compounds **8i** and **9a**; log *P* values for all of our compounds (PDF)

■ AUTHOR INFORMATION

Corresponding Authors

*E-mail: hlevine@email.uky.edu.

*E-mail: sylviegtsodikova@uky.edu.

Author Contributions

M.Y.F. performed all chemistry experiments. K.M. and E.H. performed the experiments for Figure 1. H.L. performed the experiments for Figure 2 and Table 1. S.G.T., M.Y.F., and H.L. designed experiments, analyzed data, and wrote the manuscript. S.G.T. made all final Figures.

Funding

This work was supported by startup funds from the University of Kentucky (to S.G.-T.), by NIH Grant AI90048 (to S.G.-T.), and by NIH Grant 1R21 NS080576-01A1 (to H.L.), and NIH Center Core Grant P30AG028383 (Alzheimer's Disease Center).

Notes

The content is solely the responsibility of the authors and does not necessarily represent the official views of the National Institutes of Health.

The authors declare no competing financial interest.

■ ACKNOWLEDGMENTS

We thank Dr. David S. Watt for initial compounds implicating chalcones as PIB-displacing Aβ ligands. We acknowledge Linda Van Eldik, Ph.D. Sanders-Brown Director, Peter Nelson, M.D., Ph.D., Neuropathology Core Director, and Sonya Anderson, Brain Bank Coordinator for human brain tissue and their contributions on behalf of the ADC. We are forever in debt to the patients whose brain donations made this investigation possible.

■ REFERENCES

(1) Klunk, W. E., Engler, H., Nordberg, A., Wang, Y., Blomqvist, G., Holt, D. P., Bergstrom, M., Savitcheva, I., Huang, G. F., Estrada, S., Ausen, B., Debnath, M. L., Barletta, J., Price, J. C., Sandell, J., Lopresti, B. J., Wall, A., Koivisto, P., Antoni, G., Mathis, C. A., and Langstrom, B. (2004) Imaging brain amyloid in Alzheimer's disease with Pittsburgh Compound-B. *Ann. Neurol. 55*, 306−319.

(2) Jack, C. R., Jr., Knopman, D. S., Jagust, W. J., Petersen, R. C., Weiner, M. W., Aisen, P. S., Shaw, L. M., Vemuri, P., Wiste, H. J., Weigand, S. D., Lesnick, T. G., Pankratz, V. S., Donohue, M. C., and Trojanowski, J. Q. (2013) Tracking pathophysiological processes in Alzheimer's disease: an updated hypothetical model of dynamic biomarkers. *Lancet Neurol. 12*, 207−216.

(3) Jack, C. R., Jr., Barrio, J. R., and Kepe, V. (2013) Cerebral amyloid PET imaging in Alzheimer's disease. *Acta Neuropathol. 126*, 643−657.

(4) Eckroat, T. J., Mayhoub, A. S., and Garneau-Tsodikova, S. (2013) Amyloid-beta probes: Review of structure-activity and brain-kinetics relationships. *Beilstein J. Org. Chem. 9*, 1012−1044.

(5) Lockhart, A., Ye, L., Judd, D. B., Merritt, A. T., Lowe, P. N., Morgenstern, J. L., Hong, G., Gee, A. D., and Brown, J. (2005) Evidence for the presence of three distinct binding sites for the thioflavin T class of Alzheimer's disease PET imaging agents on beta-amyloid peptide fibrils. *J. Biol. Chem. 280*, 7677−7684.

(6) Ye, L., Morgenstern, J. L., Gee, A. D., Hong, G., Brown, J., and Lockhart, A. (2005) Delineation of positron emission tomography imaging agent binding sites on beta-amyloid peptide fibrils. *J. Biol. Chem. 280*, 23599−23604.

(7) Lockhart, A. (2006) Imaging Alzheimer's disease pathology: one target, many ligands. *Drug Discovery Today 11*, 1093−1099.

(8) LeVine, H., III (2005) Multiple ligand binding sites on A beta(1−40) fibrils. *Amyloid 12*, 5−14.

(9) Klunk, W. E., Lopresti, B. J., Ikonomovic, M. D., Lefterov, I. M., Koldamova, R. P., Abrahamson, E. E., Debnath, M. L., Holt, D. P., Huang, G. F., Shao, L., DeKosky, S. T., Price, J. C., and Mathis, C. A. (2005) Binding of the positron emission tomography tracer Pittsburgh compound-B reflects the amount of amyloid-beta in Alzheimer's disease brain but not in transgenic mouse brain. *J. Neurosci. 25*, 10598−10606.

(10) Rosen, R. F., Walker, L. C., and Levine, H., 3rd. (2011) PIB binding in aged primate brain: enrichment of high-affinity sites in humans with Alzheimer's disease. *Neurobiol. Aging 32*, 223−234.

(11) Matveev, S. V., Spielmann, H. P., Metts, B. M., Chen, J., Onono, F., Zhu, H., Scheff, S. W., Walker, L. C., and LeVine, H., 3rd. (2014) A distinct subfraction of Abeta is responsible for the high-affinity Pittsburgh compound B-binding site in Alzheimer's disease brain. *J. Neurochem. 131*, 356−368.

(12) Ni, R., Gillberg, P. G., Bergfors, A., Marutle, A., and Nordberg, A. (2013) Amyloid tracers detect multiple binding sites in Alzheimer's disease brain tissue. *Brain 136*, 2217−2227.

(13) LeVine, H., 3rd. (1993) Thioflavin T interaction with synthetic Alzheimer's disease beta-amyloid peptides: detection of amyloid aggregation in solution. *Protein Sci. 2*, 404−410.

(14) Batovska, D. I., and Todorova, I. T. (2010) Trends in utilization of the pharmacological potential of chalcones. *Curr. Clin. Pharmacol. 5*, 1−29.

(15) Fosso, M. Y., LeVine, H., III, Green, K. D., Tsodikov, O. V., and Garneau-Tsodikova, S. (2015) Effects of structural modifications on the metal binding, anti-amyloid activity, and cholinesterase inhibitory activity of chalcones. *Org. Biomol. Chem. 13*, 9418−9426.

(16) Klunk, W. E., Wang, Y., Huang, G. F., Debnath, M. L., Holt, D. P., Shao, L., Hamilton, R. L., Ikonomovic, M. D., DeKosky, S. T., and Mathis, C. A. (2003) The binding of 2-(4′-methylaminophenyl)-benzothiazole to postmortem brain homogenates is dominated by the amyloid component. *J. Neurosci. 23*, 2086−2092.

(17) LeVine, H., 3rd. (1999) Quantification of beta-sheet amyloid fibril structures with thioflavin T. *Methods Enzymol. 309*, 274−284.

(18) Matveev, S. V., Kwiatkowski, S., Sviripa, V. M., Fazio, R. C., Watt, D. S., and LeVine, H., 3rd. (2014) Tritium-labeled (*E*,*E*)-2,5-bis(4′-hydroxy-3′-carboxystyryl)benzene as a probe for beta-amyloid fibrils. *Bioorg. Med. Chem. Lett. 24*, 5534−5536.

(19) Zhao, P. L., Liu, C. L., Huang, W., Wang, Y. Z., and Yang, G. F. (2007) Synthesis and fungicidal evaluation of novel chalcone-based strobilurin analogues. *J. Agric. Food Chem. 55*, 5697−700.

DOI: 10.1021/acschemneuro.5b00266
ACS Chem. Neurosci. 2016, 7, 171−176